

Impact of Electricity Price and Desalination Cost on Green Hydrogen Production from High-Salinity Seawater in the Gulf of Suez

Wael W. Eskander ^{1,*}, Moustafa A. Fouz ², Sameh Shaaban ³, and Ahmed A. Swidan ⁴

^{1,2,3} Arab Academy for Science, Technology and Maritime Transport (AASTMT), College of Engineering and Technology, Mechanical Engineering Department, Cairo, Egypt

⁴ Arab Academy for Science, Technology and Maritime Transport (AASTMT), Cairo, Egypt

⁴ University of New South Wales, Canberra, Australia

w.mesiha31005@student.aast.edu, moustafa.fouz@aast.edu, sameh.shaaban@aast.edu, ahmed.swidan@aast.edu

Abstract

Electrolytic hydrogen is a key enabler for renewable energy integration and storage, with proton exchange membrane (PEM) electrolysis offering high efficiency and operational flexibility. However, PEM systems require ultra-high-purity water, limiting the direct use of seawater, particularly in high-salinity environments. This study evaluates the technical and economic feasibility of green hydrogen production using high-salinity seawater from the Gulf of Suez (>40,000 mg/L) as feedstock for a PEM electrolyzer operating at 300 L/h.

Several desalination configurations were developed, including single-pass and double-pass reverse osmosis (RO) systems with ultrafiltration (UF) pretreatment and ion-exchange polishing. The systems were simulated using WAVE and ROSA to achieve ultrapure water quality (0.1–1 $\mu\text{S}/\text{cm}$) suitable for PEM operation. A techno-economic assessment was conducted to quantify the contribution of desalination to the levelized cost of hydrogen (LCOH).

The results show that double-pass RO reduces permeate salinity but increases overall energy consumption, chemical usage, and water cost by 10–35% compared to single-pass systems. Despite these differences, desalination contributes less than 0.2% to LCOH, with a variation below 0.02%. In contrast, electricity accounts for more than 70% of total hydrogen production cost, confirming it as the dominant cost driver. These findings demonstrate that single-pass RO with polishing is sufficient for PEM applications and that cost reduction efforts should prioritize electricity price and electrolyzer performance.

Index-words: PEM electrolyzer, Sensitivity Analysis, SWRO, Techno-economic Assessment, WAVE simulation.

I. Nomenclature

Term	Meaning
SEC_{des}	Specific energy consumption of desalination (kWh/m^3).
$C_{chem, des}$	chemical & utility cost for desal per m^3 ($\$/\text{m}^3$).
C_{water}	specific water cost ($\$/\text{m}^3$) (energy+ chemicals+ WWD+ small O&M)
$C_{stack_repl, ann}$	annual stack replacement cost for electrolyzer ($\$/\text{yr}$).
C_{wwdisp}	wastewater disposal cost per m^3 ($\$/\text{m}^3$)

$Q_{des, ann}$	annual desalinated volume used by the electrolyzer (m^3/yr).
$C_{membr, ann}$	annual membrane replacement + amortized membrane CAPEX ($\$/\text{yr}$)
$C_{elec_O\&M, ann}$	annual electrolyzer fixed O&M ($\$/\text{yr}$).
$CAPEX_{elec}$	electrolyzer capital cost ($\$$).
$CAPEX_{des}$	desalination capital cost attributable to water for electrolysis ($\$$).
$C_{chem, des}$	chemical & utility cost for desal per m^3 ($\$/\text{m}^3$).

II. Highlights

- Assessment of the cost of desalination processes in relation to the total hydrogen production costs.

- Investigation of the applicability of offshore hydrogen production from seawater.
- To assess the green hydrogen production potential offshore.

* Corresponding author

III. Introduction

The rapid growth in global energy demand, coupled with escalating greenhouse gas emissions and deteriorating air quality, has intensified the need for a transition toward low-carbon and sustainable energy systems. In the context, green hydrogen has emerged as a key energy vector capable of enabling decarbonization across power generation, industrial processes, and transportation sectors. Despite the validity and potential, the large-scale deployment of electrolytic hydrogen production is strongly dependent on the availability of ultra-high-purity water. This factor poses a significant challenge for arid and semi-arid coastal regions in Egypt, where freshwater resources are scarce despite the abundance of seawater [1].

Proton exchange membrane (PEM) electrolysis (Fig. 1) is widely regarded as one of the most efficient and flexible technologies for green hydrogen production due to its high current density, rapid response, and compact design [2]. However, several works have highlighted that electrolysis-based hydrogen production requires ultra-high-purity water, making desalination an essential upstream process when seawater is used as a feedstock and extremely low electric conductivity to prevent membrane degradation and ensure long-term operational stability. Recent studies have increasingly focused on the integration of seawater desalination with hydrogen production systems to address water scarcity constraints in green hydrogen deployment. At the same time, direct seawater electrolysis has been investigated as an alternative pathway; however, it faces significant technical challenges, including chloride-induced corrosion, competing chlorine evolution reactions, and system instability, which limit its large-scale applicability.

Recent studies have increasingly focused on the integration of seawater desalination with hydrogen production systems and the techno-economic drivers governing the Levelized Cost of Hydrogen (LCOH), [3] reviewed seawater treatment technologies for electrolysis, emphasizing the necessity of multi-stage purification to meet stringent water quality requirements, [4] highlighted that electrolysis energy consumption dominates overall system energy demand, while desalination contributes only a minor fraction. Similarly, [5] investigated integrated desalination–electrolysis systems and demonstrated that optimization of system configuration and energy inputs is critical

for reducing hydrogen production cost. These recent contributions confirm that while desalination is essential for enabling seawater-based hydrogen production, electricity cost and electrolyzer performance remain the primary determinants of LCOH.

Recent techno-economic studies have shown that the integration of desalination and hydrogen production can be optimized through system-level design, where parameters such as electrolyzer efficiency, energy consumption, and system configuration strongly influence overall performance and cost.

For instance, [6] introduced a fuzzy VIKOR-based approach for evaluating hydrogen technologies, while [7] explored the strategic potential of Egyptian ports as green energy logistics hubs

Despite these advances, most existing studies focus either on electrolysis performance or on desalination technologies independently, with limited work addressing the combined techno-economic evaluation of desalination configurations under high-salinity conditions.

Reverse osmosis (RO) is currently the dominant desalination technology due to its comparatively low energy consumption and high salt rejection.

Numerous studies have investigated the techno-economic performance of RO systems, demonstrating that the optimal design of single-stage and multi-stage seawater RO systems is highly sensitive to operating parameters and cost factors. [8] showed that RO systems outperform alternative desalination technologies in terms of energy efficiency. [9] Reported that adding a second RO stage can significantly enhance water recovery; however, small-scale RO systems without energy recovery may consume two to three times more energy. The impact of feedwater temperature has also been highlighted. [10] showed that higher temperatures increase both permeate flux and membrane fouling, which is particularly relevant for hot climate operation.

Under Egyptian climatic conditions, the operation of seawater RO systems presents unique challenges. [11] emphasized the necessity of optimizing RO performance under hot conditions, also [12] showed that desalination cost varies seasonally and geographically across Egypt, with the highest cost

occurring at the Gulf of Suez due to elevated salinity and temperature. Despite this, most previous studies have not addressed ultra-purification systems for PEM electrolyzers under high-salinity Red Sea conditions.

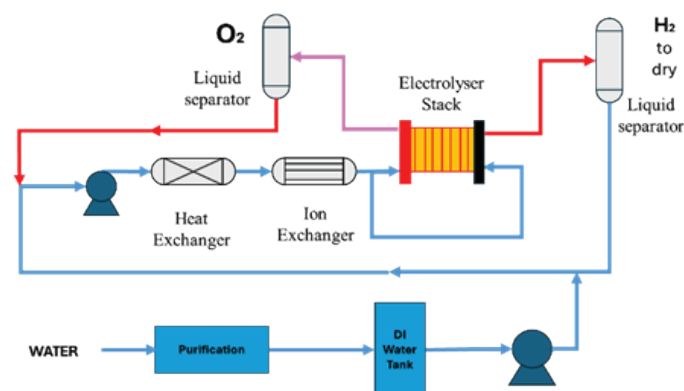


Figure 1: Proton exchange membrane (PEM) electrolysis system.

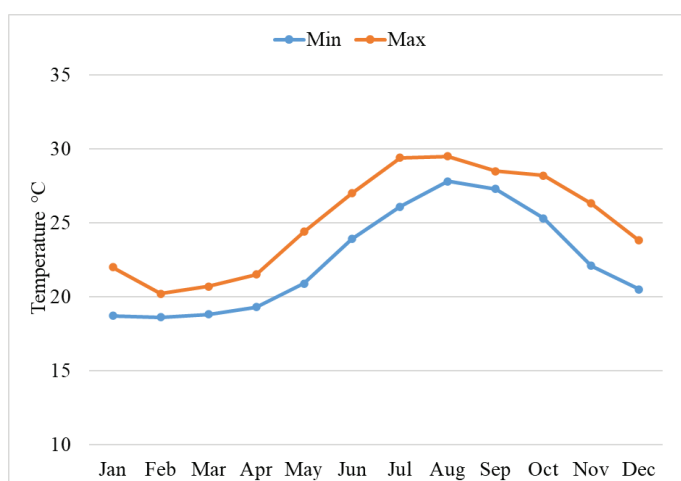


Figure 2: Monthly average max/min water temperatures. (sea temperature.org 2025)

In particular, limited studies have systematically compared multiple desalination configurations under high-salinity conditions using consistent process simulation and cost modeling, which motivates the present 24-case comparative assessment. However, comparative assessments of single-pass and double-pass RO systems integrated with PEM electrolysis under extreme salinity environments remain scarce. Moreover, the combined influence of desalinated water cost and electricity price on the levelized cost of hydrogen (LCOH) under realistic high-salinity conditions is still needed.

On the hydrogen side, recent studies have explored electrochemical hydrogen production from seawater; however, comprehensive techno-economic assessments remain limitedly investigated [13]. Laboratory-scale hydrogen production using seawater electrolytes, while [14] highlighted critical gaps in the literature, including the limited focus on commercial feasibility and the scarcity of sensitivity analyses.

Unlike previous studies, which primarily focus on either electrolysis performance or desalination technologies in isolation, this study addresses the above gap by providing a detailed techno-economic comparison of single-pass and double-pass RO desalination configurations integrated with PEM electrolysis under high-salinity conditions representative of the Gulf of Suez.

This work combines detailed process simulation (WAVE/ROSA) with LCOH analysis to quantify the relative contribution of desalination to hydrogen production cost. The novelty of this study lies in (i) the systematic evaluation of 24 desalination configurations using WAVE simulation, (ii) the direct quantification of desalination energy and cost contributions to LCOH, and (iii) a sensitivity analysis demonstrating the relative dominance of electricity cost over water treatment cost. This approach provides new insights into the role of desalination in large-scale green hydrogen production from seawater. The study further evaluates system-level trade-offs between energy consumption, water cost, and operational complexity, providing practical design insights for coastal hydrogen production systems.

Although previous studies have established that electricity cost is the dominant contributor to LCOH in PEM electrolysis systems, the impact of desalination system design under high-salinity conditions remains insufficiently quantified. The novelty of this work lies in providing a systematic comparison of 24 desalination configurations, enabling the identification of design thresholds beyond which additional process complexity does not result in meaningful economic improvement.

In particular, this study demonstrates that while double-pass RO systems improve specific energy consumption, they introduce higher overall energy demand, chemical usage, and operational complexity without reducing LCOH. This finding provides a practical design insight: for high-salinity

seawater applications, system simplicity (single-pass RO with polishing) is more economically favorable than incremental efficiency improvements achieved through multi-stage desalination.

IV. Methodology & System design

The methodology adopted in this study consists of three main stages: (i) system design and configuration selection, (ii) process simulation and performance evaluation, and (iii) techno-economic assessment. First, multiple desalination configurations, including single-pass and double-pass RO systems integrated with UF pretreatment and ion-exchange polishing, were developed based on commercially available components. Second, the performance of each configuration was simulated using WAVE and ROSA software under site-specific operating conditions representative of the Gulf of Suez. Finally, the levelized cost of hydrogen (LCOH) was calculated by integrating desalination energy consumption, chemical usage, and electrolyzer performance within a unified economic framework.

A. System design and configuration selection

The Gulf of Suez is selected as a representative high-salinity environment, and its key hydrographic and operational characteristics are considered qualitatively to contextualize the system design.

1. Local boundary conditions: Gulf of Suez:

The design and performance of seawater desalination systems are strongly influenced by site-specific boundary conditions. In the present study, Fig. 2 reports an annual sea surface temperature range between approximately 21.91 °C and 29.22 °C, throughout the year, with higher temperatures during summer months. Elevated temperatures reduce seawater viscosity and can enhance membrane permeability; however, they also accelerate biofouling and scaling kinetics, potentially increasing chemical consumption and cleaning frequency. The results are summarized in Table 1(A).

Salinity and total dissolved solids (TDS) levels in the Gulf of Suez are among the highest globally, typically ranging from approximately 38,700 to 42,700 mg/L. Seasonal variability in TDS is primarily driven by evaporation, which is intensified under high ambient temperatures and limited freshwater

inflow. Although the variation is moderate compared to temperature fluctuations, it remains significant for RO design, as higher TDS increases osmotic pressure and requires operating pressure.

In addition, coastal conditions in the Gulf of Suez may promote biofouling due to the presence of organic matter, microorganisms, and suspended particulates. These factors necessitate robust pretreatment, such as ultrafiltration (UF), to maintain a silt density index (SDI) below 3 and ensure stable RO operation.

In this study, these boundary conditions are incorporated implicitly through the selected feedwater properties and conservative design parameters (flux and recovery).

However, short-term fluctuations and extreme events are not explicitly modeled and represent a potential source of operational variability that should be addressed in future work. The adopted temperature and salinity ranges are consistent with reported measurements for the Red Sea region [15].

2. Fouling and pretreatment considerations:

In high-salinity coastal environments such as the Gulf of Suez, operational performance is not governed solely by membrane selection and energy efficiency, but also by feedwater quality variability, including biofouling potential and suspended particulate matter. These factors can significantly influence system uptime, cleaning frequency, and chemical consumption.

To address these challenges, the proposed system incorporates ultrafiltration (UF) pretreatment to reduce turbidity and maintain silt density index (SDI < 3), thereby protecting the RO membranes from rapid fouling. In addition, conservative design parameters, including moderate flux and recovery limits, were adopted to minimize fouling and scaling risks.

Nevertheless, it is acknowledged that fouling-related operational costs, including chemical cleaning, downtime, and maintenance, may exceed membrane-related costs under certain site conditions. Therefore, while the present techno-economic analysis captures average chemical and utility costs, site-specific fouling behavior and seasonal variability should be considered in detailed design and future work.

3. Desalination system design:

The desalination system was designed using a structured, simulation-driven approach to ensure consistency across all evaluated configurations. Initially, representative seawater conditions (temperature and TDS) were defined for the selected locations. Based on these inputs, multiple desalination configurations were generated, including single-pass (SP) and double-pass (DP) RO systems integrated with UF pretreatment and ion-exchange polishing.

The process performance was simulated using WAVE and ROSA software to determine key outputs, including permeate flow rate, recovery ratio, specific energy consumption (SEC), and chemical demand. The design permeate flow rate was fixed at 300 L/h to match the PEM electrolyzer requirement.

Subsequently, system sizing was performed using flux-based design equations to calculate the number of membrane elements and pressure vessels, while ensuring operation within manufacturer-recommended limits. The UF system capacity was determined based on the RO recovery to maintain mass balance consistency.

Finally, the simulated performance outputs were integrated into the techno-economic model to calculate water production cost and Levelized Cost of Hydrogen (LCOH), enabling direct comparison between configurations.

4. RO modeling assumptions:

The reverse osmosis (RO) system was modeled using representative feedwater conditions corresponding to high-salinity seawater from the Gulf of Suez. Key parameters, including TDS, temperature, pH, and pretreatment quality (SDI and turbidity), were specified as inputs to the commercial process-simulation software (ROSA and WAVE PRO).

The RO design was based on conservative operating conditions to ensure system reliability, including a recovery ratio of 45% for single-pass systems and a staged recovery of 45% (SWRO) followed by 55% (BWRO) for double-pass configurations. Membrane flux and operating pressure were selected within manufacturer-recommended limits to minimize fouling and scaling risk. The number of membrane elements and pressure vessels was determined using flux-based design equations, ensuring

consistency with the required permeate production rate of 300 L/h. The results are summarized in Table 1(B). All simulation inputs were selected within manufacturer-recommended operating ranges to ensure practical feasibility of the proposed designs (DOW Chemical Company, 2013)[16].

Table 1: Feedwater characteristics and RO design parameters

(A) Feedwater characteristics (Gulf of Suez – Base Case)

Parameter	Value	Unit	Notes
Total Dissolved Solids (TDS)	40,000	mg/L	High-salinity seawater
Temperature	21.91 –29.22	°C	Average operating condition
pH	7.8–8.2	–	Typical seawater
Salinity	38–42	ppt	Consistent with the Red Sea
SDI (after UF)	< 3	–	UF-treated feed
Turbidity	< 1	NTU	After pretreatment

(B) RO design parameters

Parameter	Single-Pass (SP)	Double-Pass (DP)	Unit	Notes
RO Recovery	45%	45% (SWRO) + 55% (BWRO)	%	Fixed design
Permeate flowrate	300	300	L/h	PEM requirement
Feed flowrate	667	1211	L/h	From mass balance
Membrane type	SW30-2540	SW30-2540 + BW30-2540	–	DuPont
Flux	15	15–25	LMH	Within safe limits
Operating pressure	55–65	55–65 / 15–20	bar	SWRO / BWRO
Salt rejection	99.5–99.7%	>99.7%	%	Manufacturer data
Number of elements	8	8 + 6	–	From design calc.
Pressure vessels	1	1 + 1	–	Small-scale system

A summary of key WAVE simulation inputs and outputs for the representative configurations is presented in Table 2 to ensure transparency and reproducibility of the RO modeling.

Table 2: Wave simulation input–output summary for representative configurations

(A) Single-Pass RO (Best Case)

Category	Parameter	Value	Unit
Input	Feed flowrate	667	L/h
	Feed TDS	40,000	mg/L
	Temperature	25	°C
	Feed pressure	60	bar
	Recovery	45	%
	Membrane type	SW30-2540	–
	Number of elements	8	–
	Flux	15	LMH
Output	Permeate flowrate	300	L/h
	Brine flowrate	367	L/h
	Permeate TDS	~300–500	mg/L
	Salt rejection	~99.5	%
	SEC	2.96	kWh/m ³
	Energy consumption	1.971	kW

(B) Double-Pass RO (Best Case)

Category	Parameter	Value	Unit
Input	Feed flowrate	1211	L/h
	Feed TDS	40,000	mg/L
	Temperature	25	°C
	SWRO pressure	60	bar
	BWRO pressure	18	bar
	Recovery (SWRO)	45	%
	Recovery (BWRO)	55	%
	Membranes	SW30 + BW30	–
Output	Final permeate flow rate	300	L/h
	Total brine flow rate	911	L/h
	Permeate TDS (after SWRO)	~300–500	mg/L
	Permeate TDS (final)	< 50	mg/L
	Salt rejection	>99.7	%
	SEC	1.93	kWh/m ³
	Energy consumption	2.331	kW

5. Design criteria and case selection basis:

The water quality requirements for PEM electrolysis systems are stringent due to the sensitivity of the membrane and catalyst layers to ionic impurities.

In this study, a target conductivity range of 0.1–1.0 $\mu\text{S}/\text{cm}$ was adopted, consistent with commonly reported requirements for PEM electrolyzers and aligned with ASTM standards for high-purity water (e.g., ASTM Type II/III) and vendor technical guidelines [16]. These requirements ensure minimal ionic contamination, prevent membrane degradation, and maintain stable electrochemical performance. Accordingly, the desalination and polishing system was designed to consistently achieve this conductivity range under all evaluated configurations. In addition, system operation was constrained within manufacturer-recommended limits, including allowable membrane flux, recovery ratio (45% for single-pass SWRO and combined 45%–55% for double-pass systems), and silt density index (SDI < 3 for UF feed and SDI < 1 for RO permeate).

From a design standpoint, the permeate production rate was fixed at 300 L/h to match the electrolyzer demand, and all configurations were sized accordingly using flux-based design equations. Mass balance consistency between UF, RO, and polishing units was maintained for all cases.

Economically, the comparison was conducted using a consistent cost framework incorporating energy consumption, chemical usage, and membrane-related costs, which were subsequently integrated into the Levelized Cost of Hydrogen (LCOH) model. The preferred configuration in each category was identified as the one achieving the minimum LCOH while satisfying all operational and water quality constraints. This approach ensures that the selected optimal cases represent both technically feasible and economically competitive solutions.

The simulated water quality across each treatment stage for the representative configurations is summarized in Table 3.

Table 3: Simulated water quality across treatment stages

Stage	TDS (mg/L)	Conductivity ($\mu\text{S}/\text{cm}$)	SDI
Parameter	–	–	–
Feed	40,000	~55,000	–
UF Permeate	< 39,000	~50,000	< 3
RO Permeate (SP)	~300–500	~500–800	< 1
RO Permeate (DP-1)	~300–500	~500–800	< 1
RO Permeate (DP-2)	< 50	~50–100	< 1
Final (IX)	< 1	0.1–1.0	< 1

6. Energy accounting and system boundaries:

The reported desalination energy consumption represents the total electrical power demand of the desalination system as obtained from WAVE simulations. This includes (i) intake and pretreatment pumping associated with the UF system, (ii) high-pressure pumping for RO operation, and (iii) internal hydraulic and mechanical losses within the system.

Product water transfer to the PEM electrolyzer is not explicitly included, as its contribution is negligible at the studied production scale (300 L/h). Furthermore,

no energy recovery device (ERD) was considered in this analysis. While ERDs are commonly applied in large-scale seawater RO plants to reduce energy consumption, their implementation is less typical in small-scale systems and was therefore excluded to maintain consistency across all evaluated configurations.

Figure 3 shows the requirements of various configurations of the system components to be considered, enabling the definition of multiple design scenarios. This information was taken from a published technical manual of reverse osmosis equipment [17].

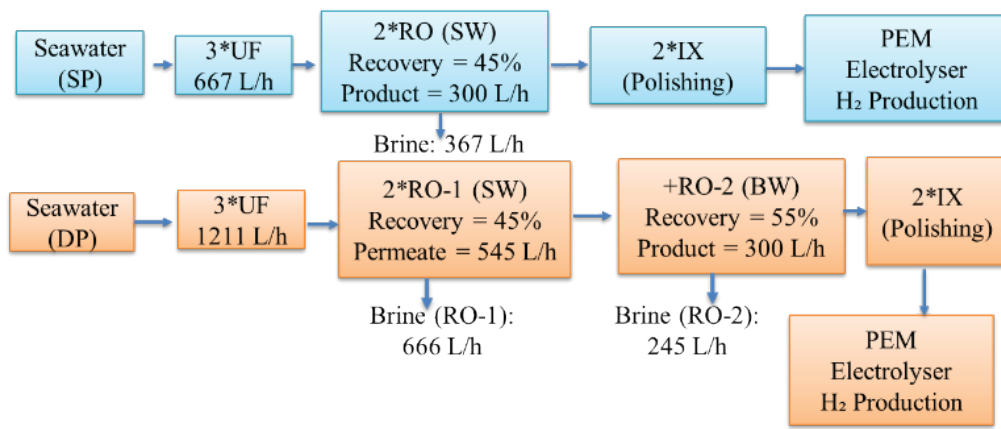


Figure 3: Single- double Pass water Desalination system configuration.

Based on the system input and the required level of treated water, three options are available for the UF module (SFP-2660, SFP-2860, SFP-2880), two options for the RO system (SW30-2540, SW30-4040), and two options for mixed-bed units (AMBERPACK, internal regeneration).

Additionally, double-pass RO configurations (SW30-2540, BW30-2540) and (SW30-4040, BW30-2540) provide further design alternatives.

Table 4: Single pass system

SP Case ID	UF	RO	IX
1	SFP-2660	SW30-2540	Mixed-bed
2	SFP-2660	SW30-2540	AMBERPACK
3	SFP-2660	SW30-4040	Mixed-bed
4	SFP-2660	SW30-4040	AMBERPACK
5	SFP-2860	SW30-2540	Mixed-bed
6	SFP-2860	SW30-2540	AMBERPACK
7	SFP-2860	SW30-4040	Mixed-bed
8	SFP-2860	SW30-4040	AMBERPACK

9	SFP-2880	SW30-2540	Mixed-bed
10	SFP-2880	SW30-2540	AMBERPACK
11	SFP-2880	SW30-4040	Mixed-bed
12	SFP-2880	SW30-4040	AMBERPACK

This means that, in total, we have 24 options (12 options for single pass RO and 12 options for double pass RO). (Table 4, 5) shows all 24 options. Initially, seawater is conveyed to the UF system, followed by high-pressure pumping to the (RO) membranes, and subsequently directed through the IX process for final purification.

7. System calculation:

The number of elements in the system is calculated as follows:

$$N_E = \frac{Q_p}{f \cdot S_E} \tag{1}$$

In equation 1, N_E is the number of elements, Q_p is the design permeate flow rate (l/hr), f is the design flux (l/m²/h), and S_E is the surface area of the element (m²). This equation is applicable to both UF and RO systems. For the UF module, the applicable feed condition could include a silt density index (SDI) of < 3, whereas for the RO permeate, the corresponding SDI requirement is < 1 [14].

Table 5: Double pass system

DP Case ID	UF	RO	IX
13	SFP-2660	SW30-2540 BW30-2540	Mixed-bed
14	SFP-2660	SW30-2540 BW30-2540	AMBERPACK
15	SFP-2660	SW30-4040 BW30-2540	Mixed-bed
16	SFP-2660	SW30-4040 BW30-2540	AMBERPACK
17	SFP-2860	SW30-2540 BW30-2540	Mixed-bed
18	SFP-2860	SW30-2540 BW30-2540	AMBERPACK
19	SFP-2860	SW30-4040 BW30-2540	Mixed-bed
20	SFP-2860	SW30-4040 BW30-2540	AMBERPACK

21	SFP-2880	SW30-2540 BW30-2540	Mixed-bed
22	SFP-2880	SW30-2540 BW30-2540	AMBERPACK
23	SFP-2880	SW30-4040 BW30-2540	Mixed-bed
24	SFP-2880	SW30-4040 BW30-2540	AMBERPACK

Thus, to determine a suitable number of elements, we should evaluate N_E for the maximum and minimum values of f and Q_p for the RO modules. In case of the UF modules, the calculations are governed by the corresponding RO recovery rate, since the UF permeate serves as the feedwater for the RO system. This methodology was also applied to the double RO system. In this study, the recovery ratio was held constant across all design options with a value of 45 % (SWRO) for single pass and 45 % (SWRO) + 55 % (BWRO) for double pass.

For the design to correctly reflect actual conditions, each element has limitations for recovery based on the allowable maximum flux by the manufacturer. Thus, the recovery factor for each element must be calculated. Practically, a single UF module is sufficient to produce 667 L/h at the typical flux ranges listed. The calculated modules are summarized in Table 6.

Table 6: Comparison of UF modules

UF Module	Membrane Area (m ²)	Typical Flux Range (LMH)	Operating Flow Range per Module (L/h)	UF Flow Required (L/h)	Calculated Modules	Modules Selected
SFP-2660	33	40 - 90	1,320 - 2,970	667	0.23 - 0.51	1
SFP-2860	51	40 - 110	2,040 - 5,610	667	0.12 - 0.33	1
SFP-2880	77	40 - 110	3,080 - 8,470	667	0.08 - 0.22	1

Equation (2) was utilized to calculate the number of pressure vessels, the number of pressure vessels (PV), is equal to the number of elements divided by the number of elements per pressure vessel, the calculated pressure vessel and element are summarized in Table 7, [18].

$$N_V = \frac{N_E}{N_{E_pV}} \quad (2)$$

B. Process simulation and performance evaluation

The analysis is based on the following key assumptions: (i) a constant hydrogen production rate corresponding to a permeate flow of 300 L/h, (ii) fixed recovery ratios of 45% for single-pass RO and 45% + 55% for double-pass configurations, (iii) steady-state operation without energy recovery devices, and (iv) electricity price and electrolyser performance parameters consistent with literature-reported values.

Table 7: Calculation of the number of RO membrane elements and pressure vessels

Element	RO Pass	Q_p (L/h)	f (L/m ² ·h)	S_e (m ²)	N_e (exact)	N_e (design)
SW30-4040	Single Pass	300	15	7.4	2.70	3
SW30-2540	Single-Pass	300	15	2.8	7.14	8
SW30-4040	DP Pass1 (SWRO)	545	15	7.4	4.91	5
SW30-2540	DP Pass1 (SWRO)	545	15	2.8	12.98	13
BW30-2540	DP Pass2 (BWRO)	300	25	2.6	4.62	5

These assumptions ensure consistency across all evaluated configurations and enable a fair comparison of desalination system performance.

The desalination performance for all 24 configurations was calculated using the governing equation in conjunction with site-specific total dissolved solids (TDS) and temperature inputs. The economic assessment incorporates the capital expenditure (CAPEX) of the electrolyzer, stack replacement costs, and the amortized operation and maintenance (O&M) expenses.

Specific water cost (USD per m³):

$$C_{energy,des} = SEC_{des} \times P_{el} \text{ (\$/m)} \quad (3)$$

$$C_{water} = C_{energy,des} + C_{chem,des} + C_{wwdisp} + C_{membr,ann} / Q_{des,ann} + C_{other,ann} / Q_{other,ann des,ann} \quad (4)$$

where,

$C_{membr,ann}$ = annual membrane replacement + amortized membrane CAPEX (\$/year)

C_{wwdisp} = wastewater disposal cost per m³ (\$/m³)

$Q_{des,ann}$ = annual desalinated volume used by the electrolyzer (m³/year).

Table 8: Techno-economic assumptions used in LCOH analysis

Parameter	Symbol	Value	Unit	Description
Electricity price	P_{el}	0.04–0.05	\$/kWh	grid electricity cost (assumed constant)
Electrolyzer CAPEX	C_{cap}	800–1000	\$/kW	PEM electrolyzer capital cost
Stack replacement cost	C_{stack}	Included	–	Periodic replacement (included in OPEX)
Electrolyzer efficiency	η_{el}	65–70	%	Conversion efficiency (HHV basis)
Capacity factor	CF	90	%	Annual operating availability
Operating hours	t_{op}	8000	h/year	Annual operation time
Project lifetime	N	20	years	Economic lifetime
Discount rate	r	8	%	Used for annualization
Water consumption	V_w	0.009	m ³ /kg H ₂	PEM requirement
SEC (SP)	SEC_{SP}	2.96	kWh/m ³	Single-pass desalination
SEC (DP)	SEC_{DP}	1.93	kWh/m ³	Double-pass desalination
Desalination energy (SP)	E_{des}	0.027	kWh/kg H ₂	From SEC × water use
Desalination energy (DP)	E_{des}	0.017	kWh/kg H ₂	From SEC × water use
Chemical cost (SP)	–	3.004	\$/day	Best case
Chemical cost (DP)	–	4.079	\$/day	Best case

C. Techno-economic assessment of the levelized cost of Hydrogen (LCOH, USD/kg)

The Levelized Cost of Hydrogen (LCOH) was calculated using a standardized annualized cost approach, incorporating capital expenditure, electricity cost, water treatment cost, and operational expenses. The dominant contribution arises from electricity consumption, calculated as:

$$C_{el} = E_{el} \times P_{el} \tag{5}$$

where E_{el} is the energy consumption of the electrolyzer (kWh/kg H₂), and P_{el} is the electricity price (\$/kWh).

Levelized hydrogen cost (USD/kg)

$$LCOH = \frac{\text{Annual_cost}}{H_{ann}} \tag{6}$$

The total LCOH is then expressed as:

$$LCOH = \frac{C_{cap, ann} + C_{el} + C_{water} + CO\&M}{H_{ann}} \tag{7}$$

where:

$C_{cap, ann}$ is the annualized capital cost (\$/year)

C_{el} is the electricity cost (\$/year)

C_{water} is the desalination cost (\$/year)

$CO\&M$ is the operation and maintenance cost (\$/year)

H_{ann} is the annual hydrogen production (kg/year).

All assumptions used in the calculation are summarized in Table 8 to ensure reproducibility

normalized metric, Desalination Energy (kWh/kg H₂) defined as:

$$Edes, kg = \frac{Edes, day}{H_{day}} \tag{8}$$

where,

$$H_{day} = 4.8 \text{ kg H}_2/\text{day}.$$

D. Study Workflow

The overall methodology adopted in this study is summarized as a sequential workflow. The analysis begins with the characterization of seawater

conditions at the Gulf of Suez, including temperature and total dissolved solids (TDS). Based on these conditions, multiple desalination configurations are defined, including single-pass and double-pass reverse osmosis (RO) systems integrated with ultrafiltration (UF) pretreatment and ion-exchange (IX) polishing.

Subsequently, each configuration is simulated using WAVE and ROSA software to determine permeate quality, recovery, energy consumption, and chemical usage. The number of membrane elements and pressure vessels is then calculated using design equations based on flux and membrane surface area constraints.

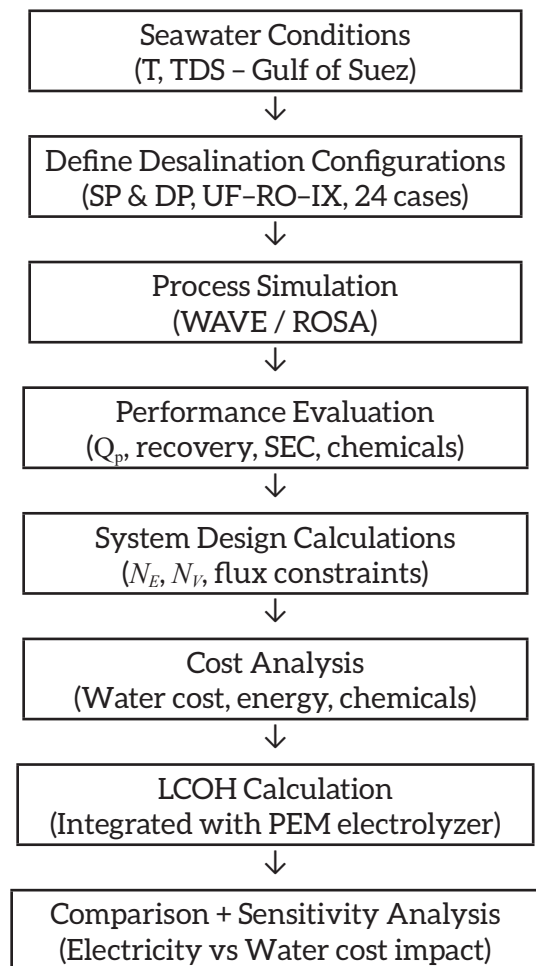


Figure 4: Methodological workflow for integrated desalination and hydrogen production assessment.

The obtained performance parameters are used to evaluate the desalination-specific cost components, including energy, chemicals, and membrane replacement. These costs are integrated with electrolyzer parameters to calculate the Levelized Cost of Hydrogen (LCOH) for each configuration.

Finally, a comparative assessment is conducted between all configurations, followed by a sensitivity analysis to quantify the influence of key parameters such as electricity price, electrolyzer efficiency, and desalinated water cost on LCOH. The overall methodological workflow is illustrated in Fig. 4 to enhance clarity and reproducibility.

V. Results & Discussion

A. Performance of the single-Pass desalination train

The single-pass (SP) desalination configurations consistently demonstrated lower operational costs and energy demand compared to double-pass alternatives. The optimal SP configuration (Case 2) SFP-2660 UF module, SW30-2540 RO element, and AMBERPACK ion-exchange achieved a water production cost of 0.5846 \$/m³, corresponding to 0.005261 \$/kg H₂, with a total desalination energy demand of 47.304 kWh/day.

The relatively low cost is primarily attributed to the elimination of the second RO stage and the reduced chemical consumption (3.004 \$/day). In addition, the SP configuration operates at a recovery of 45%, which maintains a balance between permeate production and scaling risk while ensuring stable operation within manufacturer-recommended limits.

These results indicate that a properly optimized single-pass system is sufficient to meet the ultra-high purity requirements of PEM electrolysis without requiring additional treatment stages. (Table 3) shows the analysis of the results from employing the twelve single-pass configurations (Cases 1-12). Moreover, generally, systems incorporating the SFP-2660 UF module exhibit a marginal advantage over SFP-2860 and SFP-2880 modules, due to their lower pretreatment chemical requirements and improved filtrate quality. (Case 2) emerges as the best option among the studied single-pass configurations both economically and from a practical engineering perspective.

B. Performance of the double-pass desalination train

The double-pass (DP) desalination configurations

(Table 4), (Cases 13-24) exhibit higher operating costs than the corresponding single-pass systems, primarily due to the inclusion of an additional RO stage and the associated increase in chemical consumption for membrane cleaning and polishing. Among the evaluated double-pass configurations, Case 14, comprising the sequence of (case 14), comprising SFP-2660, SW30-2540, then BW30-2540, and finally with AMBERPACK, demonstrated the most favorable overall performance. This configuration achieved the lowest water production cost of 0.6443 \$/m³, outperforming all other double-pass cases by approximately 0.6% relative to the next best alternative (0.6483 \$/m³).

This trend is consistent with the observations obtained for the single-pass configurations, where the AMBERPACK ion-exchange polishing unit consistently delivered lower and more stable purification costs compared to mixed-bed IX systems.

The superior performance of AMBERPACK is attributed to its higher ion-exchange efficiency and reduced regeneration demand. Moreover, this performance advantage aligns well with the stringent water-quality requirements of PEM electrolyzers, reinforcing the suitability of the Case-14 configuration for high-purity hydrogen production applications under high-salinity feedwater conditions.

C. Comparative assessment of single-pass vs double-pass systems

Figure 5 shows a direct comparison between the optimal SP and DP configurations, revealing clear quantitative differences. The most significant quantitative outcome of this study is the clear distinction between single-pass (SP) and double-pass (DP) desalination systems in terms of cost and energy performance. The optimal SP configuration achieved a water cost of 0.5846 \$/m³, whereas the best DP configuration reached 0.6443 \$/m³, representing an increase of approximately 10.2%. In parallel, the total desalination energy demand increased from 47.304 to 55.944 kWh/day, corresponding to an 18.3% increase for DP systems. Chemical consumption also increased by approximately 35.8% (from 3.004 to 4.0796 \$/day), confirming that the additional RO stage introduces a measurable operational penalty.

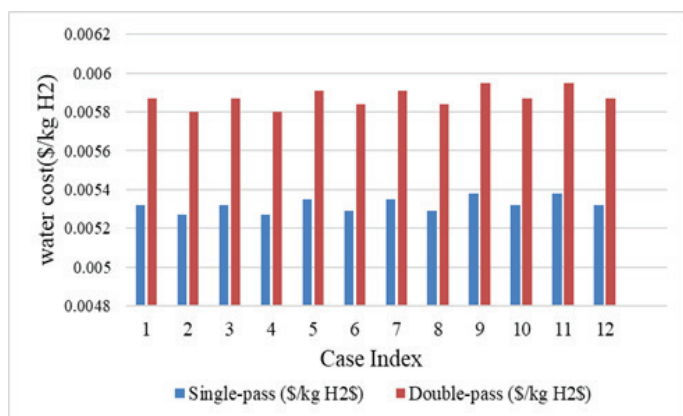


Figure 5: Comparison between the single-pass (SP) configuration and the double-pass configuration (DP).

Despite this higher total energy demand, the specific energy consumption (SEC) of DP systems (1.93 kWh/m³) is lower than that of SP systems (2.96 kWh/m³), due to improved permeate recovery. However, this reduction does not translate into a lower overall cost due to the increased system complexity and higher feed flow requirements.

From a practical standpoint, the SP configuration already achieves the required water quality for PEM electrolysis after polishing (≤ 1 μ S/cm), making DP systems unnecessary under the studied conditions. Therefore, DP configurations are only justified for extreme salinity conditions or when additional system redundancy is required.

Incorporating ERDs could reduce the absolute energy consumption of both configurations; however, the relative comparison between single-pass and double-pass systems is not expected to change significantly.

All reported economic indicators are directly traceable to physically simulated process outputs, ensuring full consistency between system design, energy consumption, and cost evaluation.

(Table 9) shows a comparison between the most favorable single-pass (SP) configuration and the highest performing double-pass configuration (DP).

D. Levelized cost of hydrogen results

(Figs. 6 and 7), shows that the impact of desalination configuration on hydrogen production cost is minimal. Despite these differences at the desalination level, the impact on hydrogen

production cost remains negligible. The LCOH varies only from 3.008526 to 3.009064 \$/kg H₂, corresponding to a difference of approximately 0.018%, clearly demonstrating that desalination configuration has a minimal influence on the overall economics. This is further supported by the fact that water cost contributes only ~0.005–0.006 \$/kg H₂, whereas electricity cost contributes approximately 2.173 \$/kg H₂, accounting for more than 70% of the total LCOH. This negligible variation confirms that desalination cost contributes only a minor fraction to the total hydrogen production cost.

From a practical perspective, these findings indicate that optimizing desalination beyond a certain threshold yields diminishing economic returns in hydrogen production systems. Instead, priority should be given to reducing electricity cost and improving electrolyzer performance. The results also suggest that single-pass desalination is sufficient for most coastal hydrogen production applications, provided that appropriate polishing (e.g., ion exchange) is implemented to meet PEM water quality requirements. Double-pass systems may still be justified in niche scenarios involving extremely high salinity or when additional operational redundancy is required.

Table 9: Best-case summary (SP vs DP)

Item	Single-Pass (SP) optimum case 2	Double-Pass (DP) optimum case 14
Configuration	SFP-2660 → SW30-2540 → AMBERPACK	SFP-2660 → SW30-2540 → BW30-2540 → AMBERPACK
Power (kWh/d)	47.304	55.944
UF Feed Flow (L/h)	667	1211
Specific Energy Consumption, SEC (kWh/m ³)	2.96	1.93
Desalination Energy (kWh/kg H ₂)	0.027	0.017
Water Cost (\$/m ³)	0.5846	0.6443
Water Cost (\$/kg H ₂)	0.005261	0.005799
Electricity Cost (\$/kg H ₂)	2.173	2.173
Chemical & Utility Cost (\$/d)	3.004	4.0796
Levelized Cost of Hydrogen, LCOH (\$/kg H ₂)	3.008526	3.009064

E. Applicability & design considerations

The results confirm that both single-pass and double-pass configurations, when combined with ion-exchange polishing, are capable of achieving the required conductivity range (0.1–1.0 $\mu\text{S}/\text{cm}$), ensuring compatibility with PEM electrolyzer operation.

Although the single-pass (SP) configuration was identified as the most economically favorable option under the conditions investigated in this study, double-pass (DP) desalination may still be required in specific practical scenarios. In particular, DP configurations become necessary when feedwater salinity or total dissolved solids (TDS) exceed typical seawater ranges (e.g., >45,000 mg/L), or when more stringent water quality targets must be achieved prior to polishing, such as in systems with highly sensitive electrolyzer components or limited polishing capacity. DP systems may also be preferred in cases where additional operational redundancy, improved permeate stability, or enhanced protection against fouling and scaling is required.

Higher temperature and salinity conditions characteristic of the Gulf of Suez slightly increase energy demand and fouling potential; however, their impact on LCOH remains limited compared to the electricity cost.

The comparison of 24 configurations shows that increasing system complexity (e.g., double-pass RO) leads to a higher operational burden without economic benefit, indicating that desalination is not the limiting factor in hydrogen production cost. This shifts the design focus from maximizing desalination efficiency to minimizing system complexity and operational cost.

While the relative trends observed in the minor contribution of desalination cost and the dominant influence of electricity cost, particularly, are expected to remain valid at larger scales, absolute cost values may vary depending on plant size, site-specific conditions, and system integration strategies. Therefore, scaling effects, economies of scale, and integration with grid energy systems should be considered in future work to generalize the findings for industrial-scale applications.

F. The sensitivity of LCOH to each parameter

The selected perturbation ranges for the sensitivity analysis were chosen to reflect realistic short-term variations and uncertainties commonly reported in techno-economic studies of hydrogen production systems. Specifically, the electricity price variation ($\pm 10\%$) represents typical market fluctuations in renewable energy pricing, particularly in regions with variable solar and wind resources. The reduction in electrolyzer efficiency (-10%) accounts for performance degradation, operational variability, and non-ideal system conditions. Similarly, the capacity factor reduction (-10%) reflects potential downtime, intermittency of renewable energy supply, and maintenance-related constraints.

The increase in electrolyzer CAPEX ($+10\%$) represents uncertainties in capital cost projections, especially given the evolving nature of electrolyzer technologies and supply chains. In contrast, a wider variation range was applied to the desalinated water cost ($+100\%$) to evaluate an extreme-case scenario, ensuring that its potential impact on the Levelized Cost of Hydrogen (LCOH) is fully captured despite its relatively small contribution.

It should be noted that these ranges are intentionally conservative and intended to capture near-term uncertainties rather than long-term variability. A more comprehensive uncertainty analysis, including probabilistic or Monte Carlo approaches, is recommended as future work to further quantify the combined impact of multiple interacting parameters.

The sensitivity analysis was designed to capture the impact of key techno-economic uncertainties on the Levelized Cost of Hydrogen (LCOH) using a structured deterministic approach. (Fig. 8) indicates that the selected perturbation ranges represent realistic deviations observed in energy markets and electrolyzer performance. Electricity price variation ($\pm 10\%$) reflects short-term fluctuations in renewable electricity cost, while reductions in electrolyzer efficiency (-10%) and capacity factor (-10%) account for operational variability, degradation effects, and intermittency of renewable energy sources. The increase in electrolyzer CAPEX ($+10\%$) captures uncertainty in capital cost projections associated with emerging hydrogen technologies.

In contrast, a wider variation range was applied to the desalinated water cost ($+100\%$) to represent an upper-bound stress scenario and to rigorously evaluate its relative contribution to LCOH. This

approach allows for a clear comparison of parameter sensitivity while maintaining consistency across all cases.

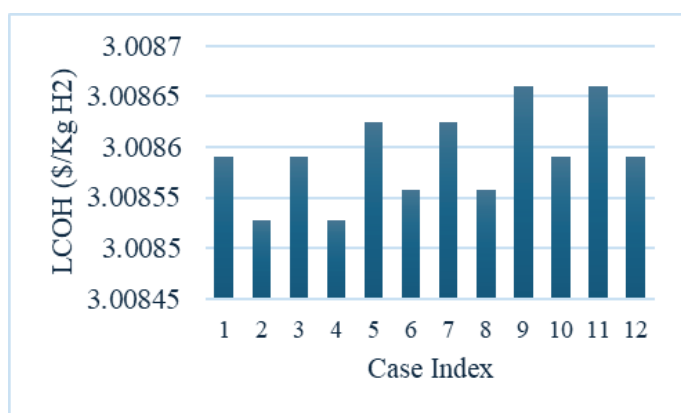


Figure 6: Effect of Single water Desalination cost on LCOH.

These variation ranges are consistent with uncertainty levels commonly reported in hydrogen techno-economic assessments and energy cost projections in the literature (International Energy Agency, 2019; International Renewable Energy Agency, 2020).

The value of the multi-case analysis lies in identifying a clear design boundary: beyond a certain level of desalination performance, further improvements in water treatment efficiency do not translate into measurable reductions in LCOH.

It is acknowledged that this approach evaluates parameters independently and does not account for potential correlations between variables. Therefore, future work should extend this analysis using probabilistic methods, such as Monte Carlo simulation or stochastic modeling, to provide a more comprehensive assessment of uncertainty and risk in integrated desalination-hydrogen systems.

VI. Conclusion

The key contribution of this study is the identification of a practical design threshold, demonstrating that increasing desalination complexity beyond a single-pass configuration does not yield economically meaningful improvements in hydrogen production cost.

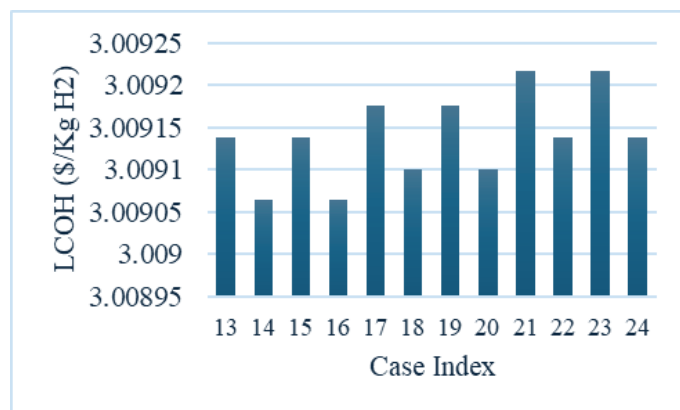


Figure 7: Effect of Double water Desalination cost on LCOH.

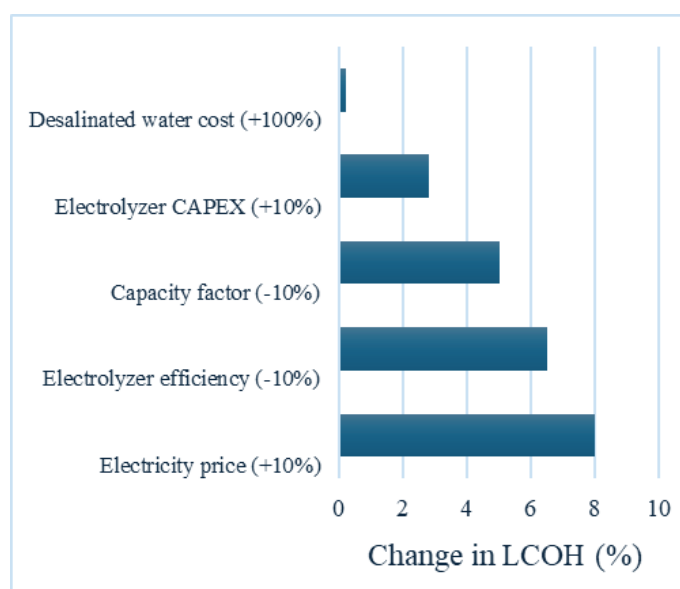


Figure 8: Parameter effect LCOH.

This study evaluated the integration of seawater desalination with PEM electrolysis for green hydrogen production under high-salinity conditions. The results demonstrate that while desalination system configuration influences water cost and energy consumption, its overall impact on the Levelized Cost of Hydrogen (LCOH) remains negligible. Electricity cost was identified as the dominant factor, contributing more than 70% of total LCOH, whereas desalinated water cost accounts for less than 0.2%.

From a practical perspective, the single-pass RO configuration combined with ion-exchange polishing is recommended as the most cost-effective and technically sufficient solution for PEM applications under typical seawater conditions. Double-pass systems should be considered only for extreme salinity or when enhanced operational robustness is required.

A limitation of this study is the use of deterministic sensitivity analysis for a fixed system scale (300 L/h). Future work should extend the analysis to larger-scale systems and incorporate probabilistic uncertainty methods to evaluate the combined effects of key techno-economic parameters.

This study investigated the techno-economic feasibility of green hydrogen production from high-salinity seawater using a PEM electrolyzer integrated with an optimized desalination and demineralization system. The results confirm that the system is capable of achieving the required ultra-high-purity water (0.1–1.0 $\mu\text{S}/\text{cm}$) under Gulf of Suez conditions.

The analysis demonstrates that desalinated water cost contributes only a marginal fraction (<0.2%) to the Levelized Cost of Hydrogen (LCOH), whereas electricity cost remains the dominant factor, accounting for more than 70% of total production cost. Among the evaluated configurations, the

single-pass RO system combined with ion-exchange polishing provides the most cost-effective solution, while double-pass systems introduce higher energy and chemical demand without significant economic benefit.

These findings indicate that efforts to reduce hydrogen production cost should primarily focus on electricity pricing and electrolyzer performance rather than further optimization of desalination processes. Future work should extend the analysis to larger-scale systems and incorporate probabilistic uncertainty methods to better capture the combined effects of key techno-economic parameters.

Acknowledgment

The authors gratefully acknowledge the support provided by their affiliated institutions for facilitating this research. Appreciation is also extended to colleagues whose technical discussions and feedback contributed to the development of this study.

References

- [1] International Energy Agency (IEA), "The future of hydrogen," Paris, France: IEA Publications, Jun. 2019. <https://www.iea.org/reports/the-future-of-hydrogen>
- [2] S. Siracusano, L. G. Aricò, and P. Antonucci, "PEM water electrolysis: Advances, challenges and perspectives," *International Journal of Hydrogen Energy*, vol. 45, no. 39, pp. 20699–20720, 2020.
- [3] Ł. Mika, K. Sztekler, Tomasz Bujok, P. Boruta, and Ewelina Radomska, "Seawater Treatment Technologies for Hydrogen Production by Electrolysis—A Review," *Energies*, vol. 17, no. 24, pp. 6255–6255, Dec. 2024, doi: <https://doi.org/10.3390/en17246255>.
- [4] M. Arunachalam, Y. Yoo, A. S. AlGhamdi, H. Park, and D. S. Han, "Integrating green hydrogen production with renewable energypowered desalination: An analysis of CAPEX implications and operational strategies," *International Journal of Hydrogen Energy*, vol. 84, pp. 344–355, 2024, doi: <https://doi.org/10.1016/j.ijhydene.2024.08.250>.
- [5] X. Xu, Z. Zhao, C. Song, L. Xu, and W. Zhang, "Seawater Membrane Distillation Coupled with Alkaline Water Electrolysis for Hydrogen Production: Parameter Influence and Techno-Economic Analysis," *Membranes*, vol. 15, no. 2, pp. 60–60, Feb. 2025, doi: <https://doi.org/10.3390/membranes15020060>.
- [6] F. Tamtam and A. Tourabi, "Innovative fuzzy VIKOR approach for green hydrogen technologies assessment: implications for sustainable energy development," *Renewable Energy and Sustainable Development*, vol. 11, no. 2, p. 229, Aug. 2025, doi: <https://doi.org/10.21622/resd.2025.11.2.1283>.
- [7] S. M. Mahmoud, M. Abdel Gelil, and S. El Gazzar, "Strategic assessment of Egyptian ports for green energy logistics hub: the case for Gargoub port," *Renewable Energy and Sustainable Development*, vol. 11, no. 2, p. 372, Oct. 2025, doi: <https://doi.org/10.21622/resd.2025.11.2.1551>.

- [8] A. M. Helal, A. M. El-Nashar, E. S. Al-Katheeri, and S. A. Al-Maler, "Optimal design of hybrid RO/MSF desalination plants Part III: Sensitivity analysis," *Desalination*, vol. 169, no. 1, pp. 43–60, Sep. 2004, doi: <https://doi.org/10.1016/j.desal.2004.08.006>.
- [9] M. A. Alghoul, P. Poovanaesvaran, K. Sopian, and M. Y. Sulaiman, "Review of brackish water reverse osmosis (BWRO) system designs," *Renewable and Sustainable Energy Reviews*, vol. 13, no. 9, pp. 2661–2667, Dec. 2009, doi: <https://doi.org/10.1016/j.rser.2009.03.013>.
- [10] T. Mohammadi, M. Kazemi Moghadam, and S. S. Madaeni, "Hydrodynamic factors affecting flux and fouling during reverse osmosis of seawater," *Desalination*, vol. 151, no. 3, pp. 239–245, Jan. 2003, doi: [https://doi.org/10.1016/S0011-9164\(02\)01016-0](https://doi.org/10.1016/S0011-9164(02)01016-0).
- [11] S. Shaaban and H. Yahya, "Detailed analysis of reverse osmosis systems in hot climate conditions," *Desalination*, vol. 423, pp. 41–51, Dec. 2017, doi: <https://doi.org/10.1016/j.desal.2017.09.002>.
- [12] S. Shaaban and H. Yahya, "Identification of cost and energy effective seawater membranes for use under hot climate conditions," *Water Environment Research*, vol. 94, no. 7, Jun. 2022, doi: <https://doi.org/10.1002/wer.10758>.
- [13] A. S. Kassem, A. E. Eissa, A. M. Zeineldin, S. G. Hemeda, and A. I. Omara, "ELECTROLYSIS OF SALT WATER AND ITS EFFECT ON THE PRODUCTION OF GREEN HYDROGEN," *Misr Journal of Agricultural Engineering*, vol. 0, no. 0, Aug. 2024, doi: <https://doi.org/10.21608/mjae.2024.310379.1143>.
- [14] V. Hugo, F. Pereira, L. Ferreira, Fabio Souza Toniolo, and Andréa Souza Santos, "A Systematic Study on Techno-Economic Evaluation of Hydrogen Production," *Energies*, vol. 16, no. 18, pp. 6542–6542, Sep. 2023, doi: <https://doi.org/10.3390/en16186542>.
- [15] Sea Temperature.org, "Sea water temperature data for the Red Sea (Gulf of Suez)," *Seatemperature.org*, 2020. <https://www.seatemperature.org/> (accessed Apr. 08, 2022).
- [16] DOW Chemical Company, "FILMTEC™ reverse osmosis membranes: Technical manual. USA: Dow," 2013. Accessed: Apr. 08, 2026. [Online]. Available: <https://www.filterwater.com/docs/filmtec/dow-filmtec-ro-membranes-technical-manual-609416.pdf>
- [17] DuPont Water Solutions, "Water and process solutions technical manual. DuPont," *Dupont.com*, 2021. <https://www.dupont.com/water/resources.html>
- [18] M. Verhuelsdonk, T. Attenborough, O. Lex, and T. Altmann, "Modeling the impact of using multi-port RO pressure vessels in seawater reverse osmosis desalination plants using special simulation software," *Desalination and Water Treatment*, vol. 5, no. 1–3, pp. 192–197, May 2009, doi: <https://doi.org/10.5004/dwt.2009.569>.